GENERAL SYMPOSIA | NANOTECHNOLOGY AND NANOCOMPOSITES

Influence of Coating Structure of an SiOx Barrier Coating on a PET Substrate on Water Vapor Permeation Activation Energy

J. Franke, M.O. Liedke, P. Dahmen, M. Butterling,
A. G. Attallah, A. Wagner, P. Alizadeh and R. Dahlmann

DOI: https://doi.org/10.51573/Andes.PPS39.GS.NN.1

December 2024

Influence of Coating Structure of an SiOx Barrier Coating on a PET Substrate on Water Vapor Permeation Activation Energy

J. Franke, M.O. Liedke, P. Dahmen, M. Butterling, A. G. Attallah, A. Wagner, P. Alizadeh and R. Dahlmann[1]

Abstract: The application of plasma polymerized silicon-based coatings on plastic substrates is an effective way to adjust the permeability of the substrate. However, the permeation mechanisms are yet not fully understood. Here, the activation energy of permeation can offer valuable insights. In order to understand how the activation energy of permeation depends on the coating structure, five silicon-based coatings with varying oxygen content were analyzed, which led to property modifications ranging from silicon-oxidic to silicon-organic. Positron annihilation spectroscopy was employed to characterize the free volume and quartz crystal microbalance measurements were used to determine the density of the coating. These results were compared to water vapor permeation measurements with a temperature variation in the range of 15°C to 50°C. As expected, the silicon-organic coatings do not significantly impact the permeation rates, while the silicon-oxidic coatings do exhibit a barrier effect. The density of the coatings increases for the more silicon-oxidic coatings. A coating with an unusually high oxygen to precursor ratio forms the exception in both permeation and density. The free volume appears to increase for the more silicon-organic coatings. The pore wall chemistry is also affected, hinting at a structural transition from silicon-organic to silicon-oxidic. With this approach, we aim for an in-depth understanding of the chemical structure of silicon-based thin film coatings and its influence on gas permeation through those coatings.

Keywords: PECVD, SiO_x, Coating Structure, Structural Transition, Positron Annihilation Spectroscopy

1 The authors J. Franke (jonas.franke@ikv.rwth-aachen.de), P. Dahmen, P. Alizadeh and R. Dahlmann are affiliated with the Institute for Plastics Processing (IKV) at the RWTH Aachen University in Germany. The authors M.O. Liedke, M. Butterling, A. G. Attallah and A. Wagner are affiliated with the Institute of Radiation Physics, Helmholtz-Zentrum Dresden-Rossendorf in Germany.

DOI: https://doi.org/10.51573/Andes.PPS39.GS.NN.1

Introduction

For applications such as food packaging or membranes, the gas permeability of plastics must be adjusted. This can be achieved via Plasma Enhanced Chemical Vapor Deposition (PECVD) with the use of Hexamethyldisiloxane (HMDSO) as a precursor. Depending on the process parameters, the degree of fragmentation of HMDSO can be tuned to adjust the organic content of the resulting coating. Lowering the organic content leads to silicon-oxidic coatings, referred to primarily as SiO_x, which have excellent gas barrier properties. In contrast, coatings with higher organic content do not have a significant gas barrier but show good gas separation properties for membrane applications [1]. This paper examines the structural transition from silicon-organic membrane coatings to silicon-oxidic gas barrier coatings.

Methods

PECVD Coating of PET Film and Si-Wafer Substrates

PECVD Coatings were applied with a variation of O_2 and HMDSO flow in the *Large Area Microwave Plasma System* (LAMPS) reactor, which is described elsewhere [2]. The parameter variation is shown in Table 1; the name of the coatings refers to their HMDSO:O_2 ratio. Increasing the O_2 flow in the process leads to a higher oxygen content in the resulting coating and changes its structure from silicon-organic to silicon-oxidic [3]. All coatings were carried out with a microwave peak power of 16 kW, pressure of 5 Pa, pulsation of 5/45 ms and a purging time of 20 s. Different substrates were used, each of which are each described in the following sections.

Table 1. PECVD Parameter Variation.

Coating	O_2 Flow [sccm]	HMDSO Flow [sccm]
1:0	0	20
1:1	20	20
1:5	100	20
1:10	200	20
1:100	1000	10

DOI: https://doi.org/10.51573/Andes.PPS39.GS.NN.1

Measurement of Water Vapor Transmission Rate (WVTR) and Calculation of Permeation Activation Energy

For the WVTR measurement, biaxially orientated polyethylene terephthalate (PET) film with a thickness of 12 µm by Flex Films Inc. was coated with a thickness of approximately 30 nm. Each coating was measured with a Permatran-W 700 (Ametek, Inc.) on five samples. Temperature has been varied between 15°C and 50°C in increments of 5°C. The temperature dependence of the water vapor permeability can be expressed as equation 1.

$$P(T) = P_0 * e^{-\frac{E_A}{RT}} \quad 1)$$

P_0 is the pre-exponential Arrhenius factor, E_A is the apparent activation energy of permeation, R is the ideal gas constant, and T is the absolute temperature. On an Arrhenius plot, the slope of a linear fit between the data points yields the value for E_A. This has been conducted for each sample, to subsequently determine mean and standard deviation of E_A for each coating. A change in E_A is a sign for a change in permeation mechanism and as such can yield valuable insights [4].

Determination of Coating Density

The coating mass was measured using the Quartz Crystal Microbalance (QCM) openQCM Q-1 by Novaetech Srl and corresponding 10 MHz Quartz Sensors. In a first step, each sensor's resonance frequency of the fundamental mode f_0 was determined. After coating the sensors with a thickness of approximately 100 nm, the resonance frequency was measured again, and the mass Δm_c of the coating could be determined from the frequency shift Δf using the Sauerbrey Equation (equation 2).

$$\Delta m_c = -\Delta f \frac{A\sqrt{\rho_q \mu_q}}{2f_0^2} \quad 2)$$

Here, A is the area of the coated electrode, and ρ_q and μ_q are the quartz's density and shear modulus, respectively. In a second step, measurements of the coating thickness d_c were conducted by stylus profilometry using Alpha-Step® D-600 Stylus Profiler by KLA-Tencor. The coating density ρ_c could be calculated with equation 3.

$$\rho_c = \frac{\Delta m_c}{A \cdot d_c} \quad 3)$$

DOI: https://doi.org/10.51573/Andes.PPS39.GS.NN.1

Characterization of Free Volumes via Positron Annihilation Spectroscopy

The porosity of the coating was characterized via Doppler broadening variable energy positron annihilation spectroscopy (DB-VEPAS). For this, the coatings were applied on gold-coated silicon wafers with a thickness of approx. 100 nm. DB-VEPAS measurements have been conducted at the apparatus for in-situ defect analysis (AIDA) [5]. Positrons have been accelerated and monoenergetically implanted into samples in the range $0.05\ keV \leq E_p \leq 35$, which allowed for depth profiling. After a short diffusion, they annihilate in delocalized lattice sites or localize in vacancy-like defects usually emitting two anti-collinear 511 keV gamma photons once they meet electrons. Since at the annihilation site thermalized positrons have negligible momentum compared to the electrons, a broadening of the 511 keV line is observed mostly due to momentum of the electrons. This broadening is characterized by two distinct parameters, S and W, defined as a fraction of the annihilation line in the middle (511 keV ± 0.70 keV) and outer regions (508.56 keV ± 0.30 keV and 513.44 keV ± 0.30 keV), respectively. The S-parameter is a fraction of positrons annihilating with low momentum valence electrons and scales with concentration and size of vacancy type defects.

The W-parameter approximates overlap of positron wave function with high momentum core electrons and is a fingerprint of local chemistry of the annihilation spot. Plotting S over W is helpful to examine atomic surrounding of the defect site and its size (type) [6]. A fraction of positrons, which approaches a pore, have a chance to bound to electrons from the pore wall and create each a bound positron-electron particle, the so-called Positronium (Ps). Then, the fraction of Ps, having spins of positron and electron parallel to each other, the so-called ortho-Ps (o-Ps), can residue in a pore or pore network for a defined time before the inevitable annihilation with another pore wall electron of the opposite spin, the so-called “pick-off” process. The pick-off process leads to emission of two gamma photons in contrast to o-Ps self-annihilation where 3 photons are emitted. How long o-Ps exists inside of free volumes (pores) scales with the pore size [7]. Since o-Ps annihilates with 2 photons, it will contribute to the S-parameter and can be detected using the DB-VEPAS method.

Results

Water Vapor Permeability

The temperature dependent WVTR profiles of all coatings are shown in Figure 1. The curves of the uncoated PET and the higher HMDSO:O_2 ratios down to 1:5 can barely be distinguished. Only the lowest ratios, 1:10 and 1:100, show a significant difference and as such exhibit barrier properties. While this is in accordance with experience, the 1:100 coating was anticipated to have superior barrier properties due to a higher degree of crosslinking and as a result, more glass-like barrier properties. It must be considered that this ratio is unusually low for the setup used and may

DOI: https://doi.org/10.51573/Andes.PPS39.GS.NN.1

lead to increased internal stress cracking or detachment of the coating. Also, the high uncertainty for both barrier coatings hinders interpretation of the data. On the right side of Figure 1, the corresponding Arrhenius plots are shown for all samples, which is used to determine the activation energy using equation 1.

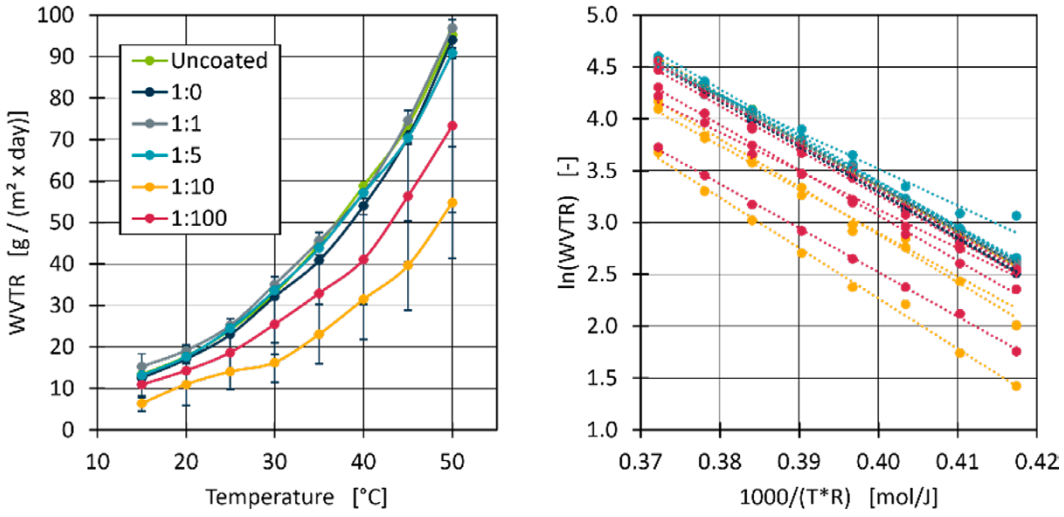

Figure 1. Measured water vapor permeation for all coatings (mean & standard deviation) over temperature (left) and corresponding Arrhenius plot where each sample is shown individually (right).

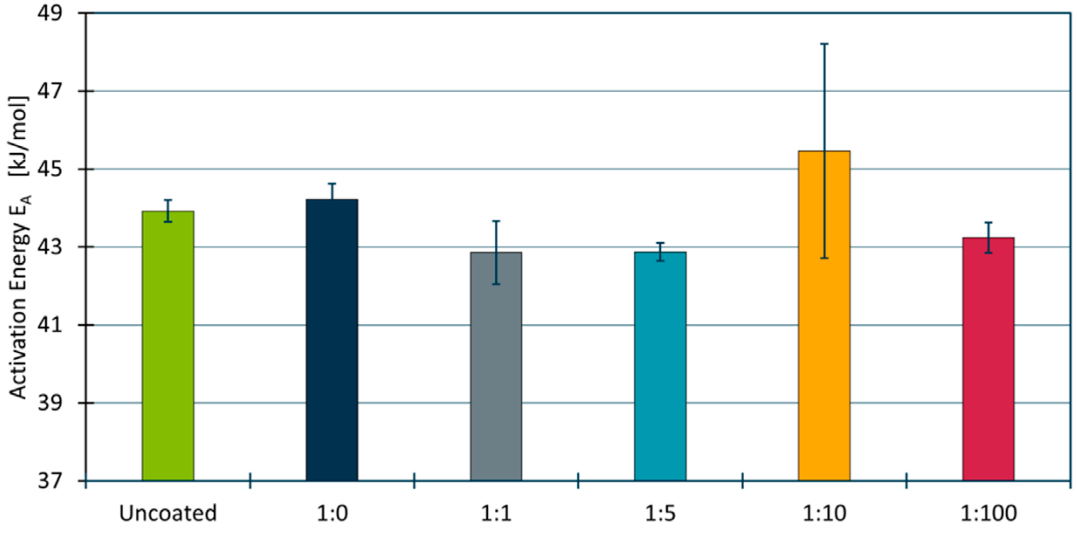

Figure 2. Calculated water vapor permeation activation energies.

As can be observed, the linear fit matches well, meaning that the samples exhibit Arrhenius behavior, and the activation energy can be calculated. The results, shown in Figure 2, suggest that the

DOI: https://doi.org/10.51573/Andes.PPS39.GS.NN.1

activation energy remains mostly the same for all coatings and the uncoated substrate, apart from the 1:10 ratio, where both mean and standard deviation are increased.

The rise in activation energy suggests that the permeation mechanism is altered for the 1:10 coating, where the permeating molecules must overcome an effective barrier coating [4]. It is remarkable that this does not occur for the 1:100 coating, which results either from internal stress cracking (see above) or an unchanged permeation mechanism.

Morphological and Chemical Structure of the Coatings

The density of the coatings determined via QCM are shown in Figure 3. A rise in density occurs with HMDSO:O_2 ratios < 1. Our hypothesis is that an increase in oxygen tends to lead to a higher degree of cross-linking in the coating, which will be examined in future studies. Once again, the 1:100 coating is noteworthy, as its density is still increased compared to higher ratios, but shows a decline compared to the ratios 1:5 and 1:10. The determination of the coating density is performed under the assumption of a homogenous coating with a constant thickness. This means that cracks in the coating that generate void volume will reduce the measured value, while the actual density is higher.

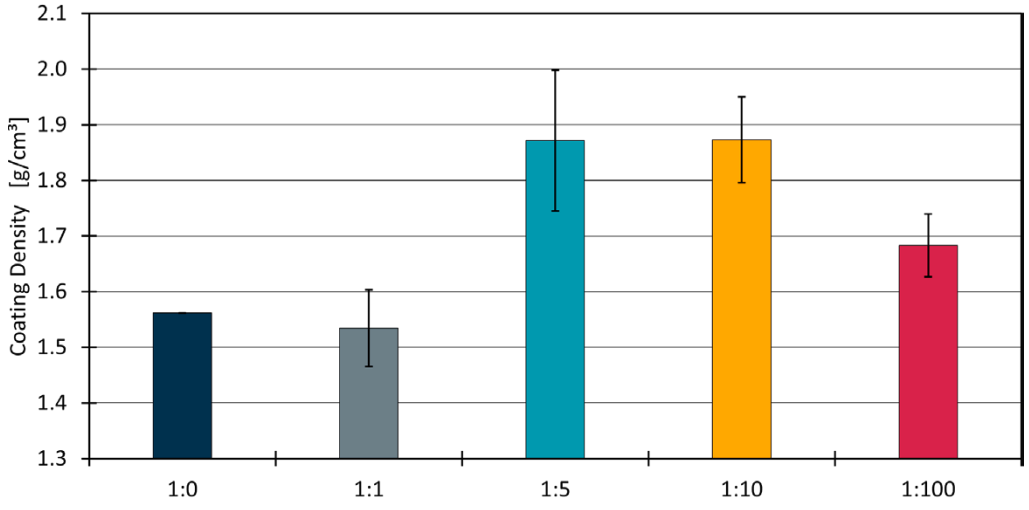

Figure 3. Calculated water vapor permeation activation energies.

Figure 4 shows the evaluated parameters S and W for vitreous carbon (C) and silica (SiO_2) as a reference, and for all coatings for implantation energies of 1.05 keV to 2.05 keV, which corresponds to implantation depths in the center of the coatings, where surface and interface effects are attenuated. The S parameter can be used as a qualitative measure for porosity, where an increase can be caused by either increased pore size or concentration. It includes, however, the other contributions

DOI: https://doi.org/10.51573/Andes.PPS39.GS.NN.1

that originate from point defects and their agglomerations. Consideration of the W parameter can yield information on the pore wall chemistry. With decreasing ratio, the coatings show a decrease in S (hence porosity) and an increase in W (corresponding to a chemical shift at the annihilation site from C to SiO_2). This suggests that the coatings are changing both in porosity and pore wall chemistry. Between ratios of 1:5 and 1:10, a structural transition seems to occur, where the porosity remains similar, while a change in pore wall chemistry is observed. This structural transition can be used to separate silicon-organic and silicon-oxidic coating structures. The silicon-organic coatings (ratios 1:0 to 1:5) exhibit a linear correlation in S-W, which is similar but less pronounced for the silicon-oxidic coatings. To illustrate this, two dashed lines are added to Figure 4 as a visual guide.

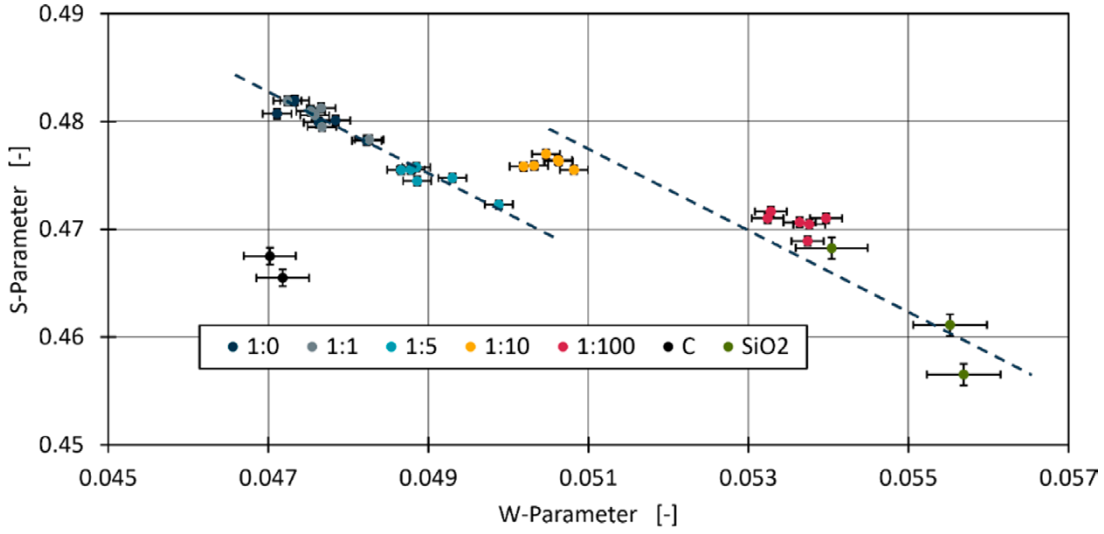

Figure 4. S-W Plot of PAS data, supplemented by reference data on vitreous carbon (C) and silica (SiO_2).

Discussion

The characterization methods in this study show different aspects of an apparent structural transition for silicon-based PECVD coatings. The highest HMDSO:O_2 ratios (1:0 and 1:1) show similar properties for WVTR (i.e., no barrier effect), E_A, density, porosity, and pore wall chemistry. It is reasonable to assume that the slight increase in oxygen flow does not significantly alter the coating structure. The 1:5 coating has the same permeation properties, but its density is increased, while porosity decreased and the pore wall chemistry is slightly shifted. This is a sign that the increase in oxygen flow starts to impact the coating structure, although no barrier effect is created. The most interesting change concerns the 1:10 coating, which constitutes the best barrier of all coatings, including an increased E_A that suggests a different permeation mechanism. While it resembles the 1:5 coating in density and porosity, the shift in pore wall chemistry seems to be the decisive factor to create an efficient gas barrier. Finally, the 1:100 coating exhibits odd behavior in almost

DOI: https://doi.org/10.51573/Andes.PPS39.GS.NN.1

all properties, which most likely results from a high degree of crosslinking that leads to high inner tensions and thus stress cracking. This affects the macroscopic WVTR and QCM measurements, whereas PAS explores the coating on a nanoscale, which is not influenced by cracks. This formation of cracks will be the subject of future studies.

Conclusion

Comprehensive research of the coating structure of silicon-based PECVD coatings with a variation of HMDSO:O_2 ratio during the process has been conducted. The coatings cover a spectrum from silicon-organic to silicon-oxidic structures, which includes a structural transition where a gas barrier effect emerges between 1:5 and 1:10. This structural transition is observed both in permeability and apparent permeation activation energy, as well as pore wall chemistry. It is not observable in density and porosity, which suggests that these properties are less important for a barrier effect, at least in this range. Further research should be conducted to confirm and better understand this structural transition.

Acknowledgments

We thank the Deutsche Forschungsgemeinschaft (DFG, German Research Foundation) for the funding of project 470287198. Parts of this research were carried out at ELBE at the Helmholtz-Zentrum Dresden-Rossendorf e.V., a member of the Helmholtz Association. We would like to thank the facility staff (Eric Hirschmann) for their assistance. This work was partially supported by the Impulse-und Net-working fund of the Helmholtz Association (FKZ VH-VI-442 Memriox), and the Helmholtz Energy Materials Characterization Platform (03ET7015).

References

1. J. Rubner et al., "On the Mixed Gas Behavior of Organosilica Membranes Fabricated by Plasma-Enhanced Chemical Vapor Deposition (PECVD)," *Membranes*, vol. 12, no. 10, 2022, https://doi.org/10.3390/membranes12100994
2. H. Behm, "Investigation of plasma processes and their influence on the composite properties of polypropylene coated by means of plasma polymerization," RWTH Aachen, 2016.
3. P. Alizadeh et al., "Stretch-tolerant PECVD gas barrier coatings for sustainable flexible packaging," *Plasma Processes and Polymers*, 2024, https://doi.org/10.1002/ppap.202400018
4. A.P. Roberts et al., "Gas permeation in silicon-oxide/polymer (SiOx/PET) barrier films: role of the oxide lattice, nano-defects and macro-defects," *Journal of Membrane Science*, vol. 208, 1-2, pp. 75–88, 2002, https://doi.org/10.1016/S0376-7388(02)00178-3

5. M.O. Liedke et al., "Open volume defects and magnetic phase transition in Fe60Al40 transition metal aluminide," *Journal of Applied Physics*, vol. 117, no. 16, 2015, https://doi.org/10.1063/1.4919014

6. M. Clement et al., "Analysis of positron beam data by the combined use of the shape- and wing-parameters," *Journal of Applied Physics*, vol. 79, no. 12, pp. 9029–9036, 1996, https://doi.org/10.1063/1.362635

7. S.J. Tao, "Positronium Annihilation in Molecular Substances," *The Journal of Chemical Physics*, vol. 56, no. 11, pp. 5499–5510, 1972, https://doi.org/10.1063/1.1677067